Level of reactive oxygen species induced by p21$^{WAF(1)/CIP(1)}$ is critical for the determination of cell fate

Takafumi Inoue,[1] Kiyoko Kato,[2] Hidenori Kato,[3] Kazuo Asanoma,[2] Ayumi Kuboyama,[1] Yousuke Ueoka,[1] Shin-ichiro Yamaguchi,[1] Tatsuhiro Ohgami[1] and Norio Wake[1,4]

[1]Department of Obstetrics and Gynecology and [2]Division of Molecular and Cell Therapeutics, Department of Molecular Genetics, Medical Institute of Bioregulation, Kyushu University, Fukuoka; and [3]Department of Obstetrics and Gynecology, National Hospital Organization Hokkaido Cancer Center, Sapporo, Japan

(Received January 12, 2009/Revised March 09, 2009/Accepted March 12, 2009/Online publication April 21, 2009)

p21$^{WAF(1)/CIP(1)}$ is a well-known cell cycle regulatory protein which is overexpressed in several cancer cell lines, and known to determine cell fate. We generated three recombinant adenovirus vectors that expressed either the full-length p21 (Ad-p21F), a p21 mutant with a deletion of the C-terminal proliferative cell nuclear antigen (PCNA) binding domain (Ad-p21N), or a p21 mutant with a deletion of the N-terminal cyclin-dependent kinase binding domain (Ad-p21C). We transfected these vectors into five cancer cell lines. Premature senescence was induced in all of the lines only following transfection with Ad-p21N and Ad-p21F. In addition, apoptosis was also induced in LoVo and HCT116 cells that harbored wild-type p53 and the reactive oxygen species (ROS) level was higher than in senescent cells. Finally, the induction of apoptosis was inhibited by using siRNA to downregulate p53. This observation implies that there is a feedback signaling loop involving p21/ROS/p53 in apoptotic responses. It appears to be, at least in part, driven by high levels of p21 protein. Next, we investigated the cell death effect of endogenous p21 protein on cell fate using sodium butyrate (NaB). Treatment with 1 mM NaB or 2 to 5 mM NaB induced senescence or apoptosis, respectively. The level of intracellular ROS in 5 mM NaB treated cells was 2-fold higher, compared with that in 1 mM NaB treated cells. We also demonstrated that DNA damage response signals including ataxia telangiectasia mutated, γH2AX, and p38 MAPK were involved in NaB-induced cell death. The magnitude of intracellular ROS levels in response to p21 elicited either senescence or apoptosis in the cancer cell lines. (*Cancer Sci* 2009; 100: 1275–1283)

Cell senescence, originally defined as the proliferative arrest that occurs in normal cells after a limited number of cell divisions, is now more broadly regarded as a general biological program of terminal growth arrest. Replicative senescence of cells due to telomeric changes exhibits similar features to those seen in DNA damage.[1,2] Therefore, DNA damage is expected to induce rapid cell growth arrest, which would be phenotypically indistinguishable from replicative senescence.[3] This type of accelerated senescence that does not involve telomere shortening is triggered in normal cells by the expression of supraphysiological mitogenic signals.[4] Not only normal cells but also cancer cells can be induced readily to undergo senescence by genetic manipulation or by treatment with chemotherapeutic agents, radiation, or differentiating agents.

The growth arrest of senescent cells is initiated by the activation of p53. Activated p53 exerts multiple effects on gene expression. In the context of senescence the most relevant is the transcriptional activation of p21, a pleiotropic inhibitor of different cyclin/CDK complexes.[5] The activation of p21 in senescent cells is only transient, and inhibitors of cyclin dependent kinase 4a (p16^{Ink4a}) become constitutively upregulated after the establishment of growth arrest.[6] The best-known mechanism for growth arrest induced by these CDK inhibitors is the blockage of CDK-mediated phosphorylation of retinoblastoma (pRb).[7] However, cell senescence, coupled with withdrawal from the cell cycle, is accelerated in the presence of sodium butyrate (NaB), even in human cervical cancer cells in which the pRb function is perturbed by the human papilloma virus (HPV) E7 oncoprotein. The induction of senescence in cervical cancer cells is not unequivocally coupled with the predominance of hypophosphorylated pRb forms.[8] This suggests the possibility that particular downstream targets of p21 that are independent of pRb-mediated signaling are able to elicit cancer cell senescence.

Reactive oxygen species (ROS), which are byproducts of normal cellular oxidative processes, are involved in senescence.[9,10] Senescent cells have higher levels of ROS than normal cells,[11] and oxidative stress caused by sublethal doses of H_2O_2 or hyperoxia can force human fibroblasts to arrest in a manner similar to senescence.[12] Additionally, both oncogenic Ras and p53 induce senescence in association with increased intracellular ROS.[13,14] p53 induces the accumulation of ROS presumably through a transcriptional influence on pro-oxidant genes.[15] In turn, p21 is capable of inducing senescence in a p53-independent manner. Up-regulation of p21 also causes increased ROS levels in both normal and cancer cells,[16] although the molecular mechanism remains unknown.

There is sufficient evidence to demonstrate a pleiotropic effect of p21, which can be inferred by its involvement in cellular differentiation, influence on gene expression and chromosomal repositioning, and the correlation of p21 expression and the efficacy of preoperative chemotherapy.[17–19] Recent evidence has suggested that p21 mediates apoptosis in a p53-independent manner,[20,21] although its role in this apoptotic pathway remains controversial. In view of the possible roles played by ROS in both senescence and apoptosis, and the capacity of p21 to elevate ROS levels, we investigated the involvement of ROS in p21-induced cell death. Additionally, we studied how the status of p21 expression modulated ROS levels to achieve alternative cell fates.

Materials and Methods

Reagent and antibodies. NaB was obtained from Wako (Osaka, Japan) and dissolved in PBS. Primary antibodies including anti-p21 polyclonal antibody (C-19 and N-20) and anti-ATM monoclonal antibody were obtained from Santa Cruz Biotechnology (Santa Cruz, CA, USA). Anti-p53 monoclonal antibody (Ab-6) and anti-phosphorylated MAPK were obtained from CalBiochem (San Diego, CA, USA). Anti-phospho-Histone 2A, X (Ser139) was obtained from Cell Signaling Technology (Beverly, MA, USA).

Cell culture. Three colorectal cancer cell lines (DLD-1, LoVo, HCT116), an ovarian cancer cell line (SKOV3), and a cervical cancer cell line (HeLa) were used in this study. LoVo cells were

[4]To whom correspondence should be addressed. E-mail: wake@med.kyushu-u.ac.jp
Abbreviations: ATM, ataxia telangiectasia mutated; CDK, cyclin-dependent kinase; DDR, DNA damage response; MAPK, Mitogen-Activated Protein Kinase PCNA, proliferative cell nuclear antigen; ROS, reactive oxygen species; siRNA, small interfering.

doi: 10.1111/j.1349-7006.2009.01166.x

cultured in F-12 Nutrient Mixture with 10% FBS at 37°C under 5% CO_2. HCT116 cells were cultured in McCoy's 5A Medium with 10% FBS. The remaining cell lines were cultured in DMEM with 10% FBS.

Vector construction and p21 infection. An adenovirus expression vector for wild-type p21 (Ad-p21F) and mutant p21 (Ad-p21N and Ad-p21C) were received as gifts from T. Furui (University of Kyushu, Fukuoka, Japan). They were constructed by ligating an EcoRI-Not fragment of human p21 cDNA into a pAxCAwt cosmid vector. 293A cells (Invitrogen, Carlsbad, CA, USA) were transfected with the pAxCAwt cosmid vector containing human p21 cDNA. The 293A transfectants were derived by limiting dilution following transfection of the pAxCAwt-p21 vector using the calcium phosphate method. A high-titer adenovirus solution was obtained from the primary lysate of a large culture of primary 293A transfectants. All cancer cell lines were infected with a MOI of approximately 20–50 for 60 min. All cell lines were analyzed after 72 h of incubation.

***N*-acetyl-L-cystein (NAC) treatment.** After NAC (Sigma, St Louis, MO, USA) was added to the medium (F-12 Nutrient Mixture and MaCoy's 5A) at a final concentration of 10 mM, LoVo and HCT116 cells were infected with p21 viral vectors described above. After 5 mM NAC was added to the medium, HCT116 cells were treated with 0.5 mM NaB.

Cell cycle analysis. Briefly, 3×10^5 cells per 6-cm plate were infected with Ad-p21 for 60 min or treated with different concentrations of NaB for 24 h; attached cells were washed twice with ice-cold PBS, and then were suspended in NP-40 lysis buffer (3.4 mM sodium citrate, 10 Mm NaCl, 0.1% NP-40) containing 0.5% propidium iodide (PI). The DNA content of the cells was measured with the FACScan (Becton Dickinson, San Jose, CA, USA) and EPICS XL (Beckman Coulter, CA, USA) systems using the PI staining method. Each fraction of the G1/S and G2/M cell phases on the DNA histograms was analyzed by CellQuest software (Becton Dickinson).

Western blot analysis. Cultured cell pellets or cancer tissues were lysed with lysis buffer containing 60 mM Tris-HCl (pH 6.8), 2% SDS, 100 mM DTT, 0.5 μg/mL leupeptin, and 0.25 mM PMSF, and boiled for 5 min. After soaking the pellets in boiling water and purifying them by centrifugation (12 000 *g* for 5 min), 15 μg of the proteins of supernatant were separated on 10–12.5% SDS-PAGE and transferred to nitrocellulose membranes. The membranes were blocked in TBS (10 mM Tris-HCl, 150 mM NaCl, 0.05% Tween 20) containing 15% non-fat dry milk at room temperature and washed in TBS-Tween for 5 min. The membranes were then incubated with diluted primary antibody. Secondary antibodies linked with HRP and blots were visualized by an enhanced chemiluminescence system (ECL; Amersham Biosciences, Buckinghamshire, UK). The amount of each protein was quantitated using NIH image software.

Aminophenyl fluorescein (APF) staining. HeLa, LoVo, and HCT116 cells were incubated with 1 μg/mL of APF (Molecular Probes, OR, USA) for 30 min, and were then washed in PBS, trypsinized, and collected in 1 mL of PBS. Fluorescence-stained cells were transferred to polystyrene tubes with cell-stainer caps (Falcon, CA, USA) and were subjected to FACS (FACScan; Beckton Dickinson) using CellQuest software (Beckton Dickinson) for acquisition and analysis.

Detection of apoptosis. LoVo and HCT116 cells were plated at a density of 2×10^4 cells/mL in two-well chamber plates (Nunc, Roskilde, Denmark) and were incubated for 24 h. After transfection with p21 viral vectors as described above, the cells were cultured for 3 days in the chamber plates. For the *in situ* apoptosis detection assay, cells were fixed in 4% formalin. Endogenous peroxidase activity was quenched with 2% H_2O_2 in PBS for 5 min. The assay was carried out according to the manufacturer's instructions (Apo-Taq *in situ* Apoptosis Detection Kit; Invitrogen).

Senescence-associated β-galactosidase (SA-β-gal) staining. Cells cultured on 6-cm dish were washed in PBS and fixed with 2% formaldehyde/0.2% glutaraldehyde in PBS for 5 min at room temperature. SA-β-gal staining was performed as described previously.[22]

siRNA transfection. p53-siRNA duplexes mixture specific to p53 (B-Bridge siTrio) and negative control siRNA were purchased from Hokkaido System Science (Hokkaido, Japan). The sequences of the sense stands are as follows: 5′-GGAAACAUUUUCAGACCUATT-3′, 5′-GCAUCUUAUCCGAGUGGAATT-3′, 5′-GAGUGCAUUG UGAGGGUUATT-3′. siRNA was carried out with LipoTrust EXOligo (Hokkaido System Science) according to the manufacturer's protocol. Briefly, HCT116 cells were plated at a density of 3×10^5 cells/mL in a 6-cm dish without antibodies and transfected with 20 nM RNA duplexes using 2 μL of LipoTrust EXOligo (Hokkaido System Science) and OPTI-MEM medium (Invitrogen). After 6 h of incubation, the medium was replaced with fresh McCoy's CA Medium with 10% FBS. Twenty-four hours later, the cells were transfected with an adenovirus expression vector carrying p21 as described above.

Statistical analysis. The statistical significance was assessed using the Mann-Whitney *U*-test and a *P*-value of less than 0.05 was considered statistically significant.

Results

The potential of p21 to induce senescence independent of its PCNA-binding function. p21 not only inhibits CDK but also acts to block DNA replication by binding to PCNA.[23,24] To evaluate which of the two functions of p21 was important for the induction of cancer cell death, we generated three types of recombinant adenovirus vectors. These vectors contained either the full-length p21 (Ad-p21F), or p21 mutants with deletions of the C-terminal PCNA binding domain (Ad-p21N), or the N-terminal CDK binding domain (Ad-p21C) (Fig. 1a,b). An adenovirus containing an empty vector (mock) was used as a control. We transferred these constructs into five cancer cell lines (SKOV3, HeLa, DLD-1, LoVo, and HCT116) using an adenovirus infection system. The cell lines were initially selected based on their susceptibility (>80%) to adenovirus (data not shown). The expression of p21 protein corresponding to the transfected vector was demonstrated by immunoblots. Both N- and C-terminal truncated proteins were detected as 14 kDa band signals (Fig. 1c).

Infection of these cancer cell lines with 20 MOI Ad-p21F and -N resulted in growth arrest, which became irreversible after 4 days. This permanent growth arrest was accompanied by the presence of a senescence-specific marker, SA-β-gal positivity, as well as morphological changes such as a dramatic increase in cell size, and enlarged and prominent nuclei (Fig. 2a). Both Ad-p21F and -N exhibited a similar potential to induce SA-β-gal-positive cells (Ad-p21F, 28–85%; Ad-p21N, 28–90%) (Fig. 2b). In contrast, no significant induction of SA-β-gal-positive cells was detected in the case of 20 MOI Ad-p21C or mock-infected cells, though abundant levels of 14 kDa signals were detectable in Ad-p21C-infected cells. These results provide evidence to support the role of the p21 CDK binding domain in the induction of cancer cell senescence.

Apoptosis induced by p21 is mediated through p53. The apoptosis of cancer cells following DNA damage is p53-dependent and yet p21-independent.[25,26] However, due to differences in the experimental conditions for investigation of the effects, contradictory conclusions have been drawn regarding the relationship between p21 and the induction of apoptosis.[27,28] In order to investigate the basis for the striking differences in the biological responses to p21 expression, we measured the kinetics of p21 protein increase, as well as its expression levels following Ad-p21F or -N infection by increasing MOI of the viral vector. Whereas 20 MOI Ad-p21 infection resulted in elongated, growth-arrested cells showing the morphological features of senescence, cells infected with 40 or 50 MOI Ad-p21 became rounded, contracted, and lost their ability to adhere to the plate with Apo-taq-positive staining (Fig. 2c). We used flow cytometry to measure the DNA contents of cancer cell

doi: 10.1111/j.1349-7006.2009.01166.x

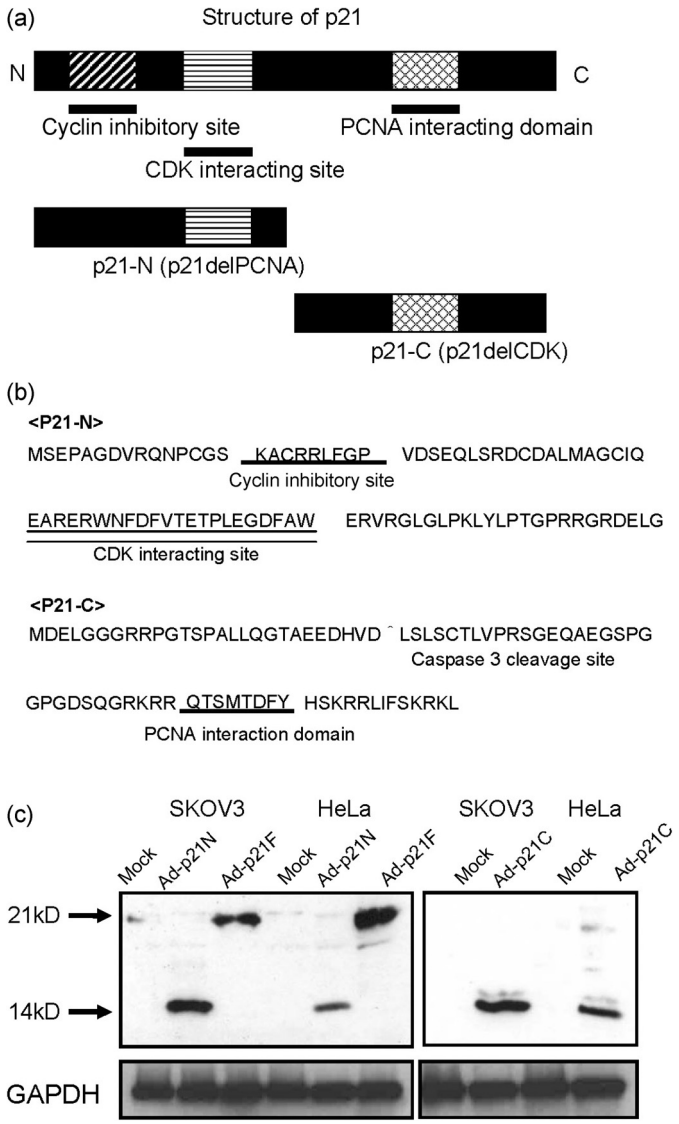

Fig. 1. Three types of recombinant adenovirus vector, Ad-p21F: wild-type full-length p21, Ad-p21N: p21 that lacks proliferative cell nuclear antigen (PCNA) binding domain, and Ad-p21C: p21 lacking cyclin-dependent kinase (CDK) binding domain, (a) and the amino-acid sequence of p21 deletion mutants are shown (b). (c) Detection of p21 protein in adenovirus transfected cells by western blots in SKOV3 and HeLa cells. All cancer cell lines were transfected with mock, Ad-p21F, Ad-p21N, or Ad-p21C, and analyzed at 76 h after infection. p21 protein was expressed in all cell lines and detected as 21 kDa as full-length bands. Mutant p21 was detected as 14 kDa bands. Each type of p21 protein (Ad-p21N or Ad-p21C) was defected by the antibody which recognized N-terminal amino acids or C-terminal amino acids, respectively.

lines following treatment with Ad-p21. In LoVo and HCT116 cells, a hypoploid peak corresponding to a subG1 population had increased following infection with Ad-p21F (40–50 MOI) (data not shown). These results are characteristic of apoptosis. The levels of p21 protein were enhanced 1.7 to 2.1-fold in LoVo cells infected with 50 MOI Ad-p21C, Ad-p21N, and Ad-p21F, compared with the 20 MOI infected cells, respectively (Fig. 2d). Infection of the cancer cells with 50 MOI Ad-mock or Ad-p21C did not induce apoptosis, indicating that adenovirus infection alone was not responsible for this effect. These two cancer cell lines harbored the wild-type *p53* gene. The levels of p53 were slightly increased with Ad-p21N (1.4-fold) and Ad-p21F (1.5-fold), compared with Ad-mock and Ad-p21C in LoVo cells. However, the level of p53 expression was not significantly different between Ad-p21F (20 MOI) and Ad-p21F (50 MOI). p53 was not detected in HeLa cells (Fig. 2e). Overexpression of p21 in response to Ad-p21 infection induced senescence in all five cancer cell lines independently of p53 status. However, overexpression of p21 could not induce apoptosis in the cell lines that harbored the mutant p53 (DLD-1 and SKOV3) or inactivated p53 by HPV E6 protein (HeLa) (data not shown). This data showed the possibility of the relationship with p53 function through the p21-induced cell death.

The fate of cancer cells as a result of ROS generated by overexpressed p21 from adenoviral transfection. To investigate the roles of ROS in the senescent or apoptotic cell fates triggered by p21 expression in LoVo and HCT116 cells, we measured ROS levels with the fluorescent probe APF,[29] a marker of changes in the general accumulation of cellular oxidants. FACS analysis of APF-stained HeLa, LoVo, and HCT116 cells revealed a progressive increase in ROS levels following 20 MOI Ad-p21F infection. After 3 days of infection, when senescent morphological changes were first observed, the ROS levels in the cells were increased more than 2-fold. We next examined whether ROS levels were involved in the decision between senescence and apoptosis in LoVo and HTC116 cells. HCT116 cells infected with 40 MOI Ad-p21F and LoVo cells infected with 50 MOI Ad-p21F exhibited much higher ROS levels (4-fold) than the cells infected with 20 MOI Ad-p21F (2 to 2.5-fold). On the other hand, the ROS levels in HeLa cells infected with 20 MOI Ad-p21F were not significantly different compared with those in cells infected with 40 MOI Ad-p21 (Fig. 3a).

We then established whether different cell fate outcomes were due to the levels of induced ROS and p21 protein. We investigated whether the antioxidant NAC could protect cells from senescent phenotypes induced by 20 MOI Ad-p21 infection or the apoptotic phenotype by 40–50 MOI Ad-p21 infection. Both LoVo and HCT116 cells that harbored the wild-type *p53* gene were infected with 20 MOI Ad p21F or -N and were cultured in the presence of 10 mM NAC for 3 days. Both Ad-p21F and -N markedly induced SA-β-gal-positive cells in the absence of NAC, and cultivation in the presence of NAC significantly suppressed the appearance of SA-β-gal-positive cells (Fig. 3b). Similarly, cultivation of LoVo and HCT116 cells in the presence of NAC for 3 days markedly inhibited apoptosis in response to 40–50 MOI Ad-p21 infection (Fig. 3c), thus suggesting that the induction of both senescence and apoptosis by p21 occurs via the generation of ROS.

The initial arrest of cell growth followed by a marked increase in the subG1 fraction in response to high titers of Ad-p21 in the cancer cells harboring the wild-type *p53* gene suggested that p53 protein was involved in the induction of apoptosis downstream of ROS accumulation. We tested this hypothesis using p53-siRNA. Treatment with p53-siRNA decreased the endogenous level of p53 in HCT116 cells. This resulted in protection from apoptotic cell death (22% to 12%) (Fig. 3d, upper panel) and the ROS levels were also lower (Fig. 3d, lower panel). These data suggest the presence of a feedback signaling loop involving elevated p21, accumulation of ROS, and p53 activation in apoptotic responses. Taken together, these findings establish that the accumulation of p21 plays a critical role in cell apoptosis that appears to be dependent on p53 status.

Endogenous p21 protein up-regulation by NaB induces cell death in colon cancer cell line HCT116 and cervical cancer cell line HeLa. Next, we investigated whether up-regulation of endogenous p21 protein has an effect similar to that of Ad-p21 infection. We have previously demonstrated that NaB induced p21 expression, resulting in growth arrest and cell death in gynecologic cancer cells.[8] To evaluate the induction of senescence in HCT116 and HeLa cells, we analyzed the cell cycle alteration and SA-β gal staining in response to NaB. We measured the DNA contents of cancer cell lines treated with varying concentrations of NaB by flow cytometry. In HCT116, treatment with 0.5 to 1.0 mM NaB resulted in a decrease in the fraction of S phase (21% to 4%) and G1 phase cells (57% to 22%). Most cells accumulated in G2/M, suggesting arrest at the G2/M

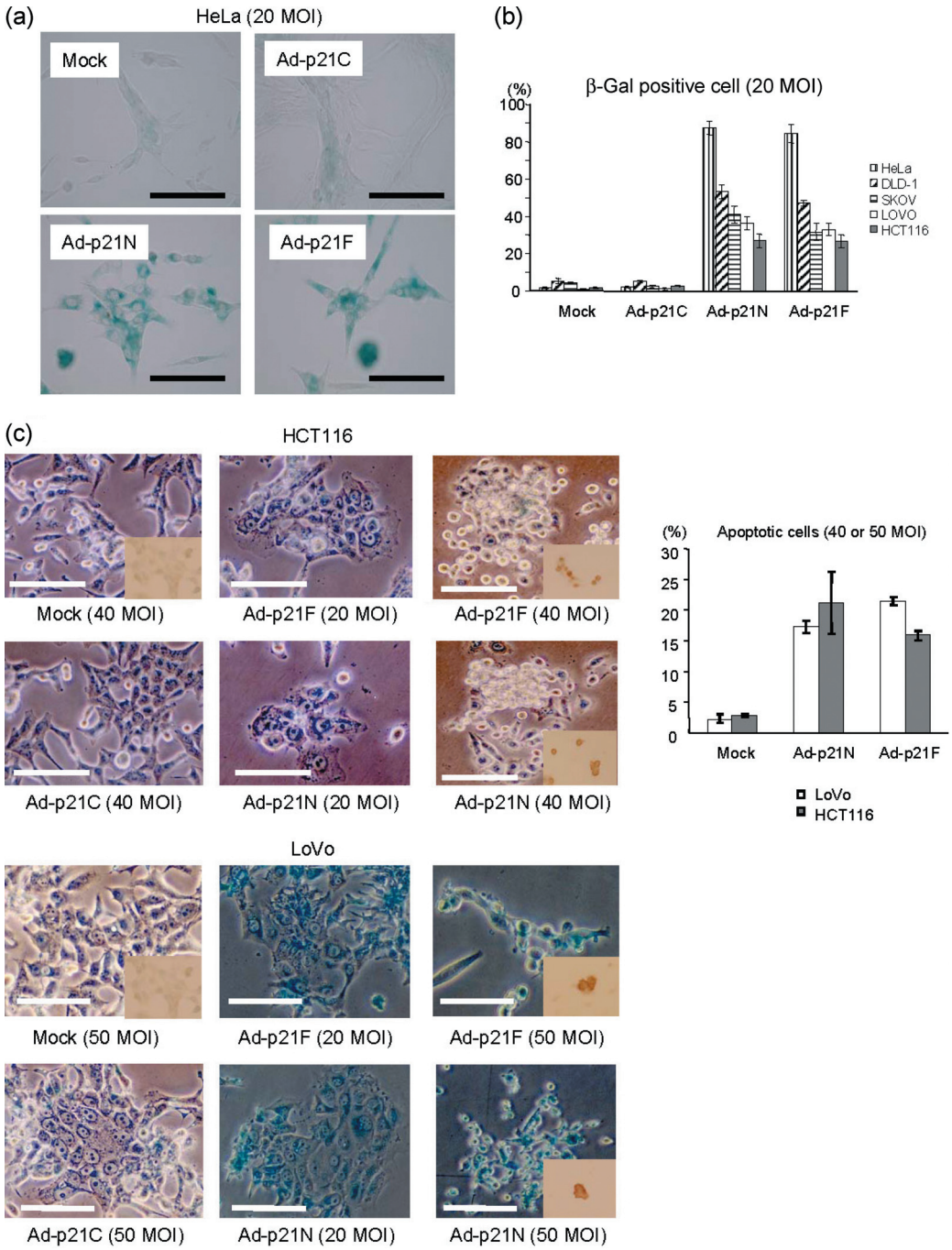

Fig. 2. Induction of senescence and apoptosis by p21 overexpression. (a) Ad-p21-N- and Ad-p21-F-infected HeLa cells were enlarged, flattened, and were senescence-associated β-galactosidase (SA-β-gal)-positive. No change in morphology was observed in cells transfected with the mock vector and Ad-p21C. Bar = 10 μM (b) The populations of SA-β-gal-positive cells (in HeLa, DLD-1, SKOV3, LoVo, and HCT116 cells) after 48 h of infection are shown. Data represent the average of three independent experiments and SD are indicated by error bars. (c) When LoVo and HCT116 cells were transfected with 20 MOI Ad-p21N and Ad-p21F, cells were enlarged, flattened, and had increased SA-β-gal positivity. At 50 MOI (LoVo) and 40 MOI (HCT116), cells were detached from the plate and floating. The small panel on the lower right for 40 or 50 MOI shows positive cells with the TUNEL assay. Mock-transfected cells showed no change in morphology and were not positive for the TUNEL assays. The populations of apoptotic cells in LoVo and HCT116 infected with 50 or 40 MOI Ad-p21 after infection of 48 h are shown in right graph as indicated by the significant increase of subG1 fraction. Data represent the average of three independent experiments and SD are indicated by error bars. Bar = 10 μM (d) Western blot of p21 expression levels in LoVo cell lysates from mock-, Ad-p21C-, Ad-p21N-, and Ad-p21F-transfected cells with different MOIs. (e) Western blot of p53 expression levels in LoVo and HeLa cell lysates from mock-, Ad-p21C-, Ad-p21N- and Ad-p21F-transfected cells with different MOIs.

doi: 10.1111/j.1349-7006.2009.01166.x

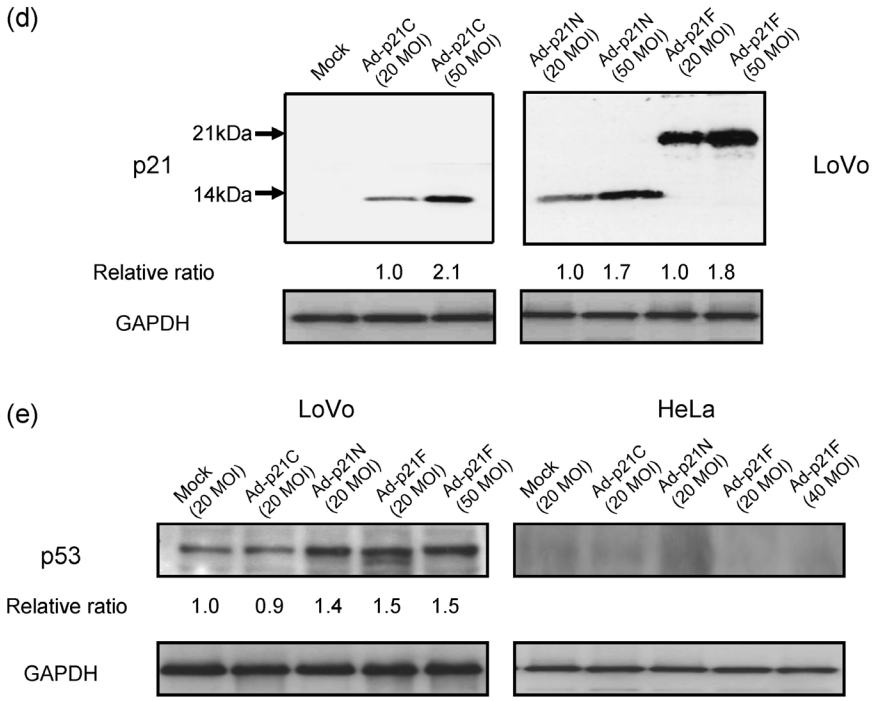

Fig. 2. *Continued*

checkpoint. A hypoploid peak corresponding to the subG1 population was evident by flow cytometry following treatment with greater than 2.0 mM NaB (Fig. 4a). This population corresponded to cells undergoing apoptotic cell death. In HeLa cells, treatment with 5–20 mM NaB resulted in a decrease in the fraction of S phase cells and accumulation at the G0/G1 phase. However, HeLa cells were resistant to apoptotic cell death by 5–20 mM NaB treatment. More than 50 mM NaB was required for the subG1 population in flow cytometry (Supplementary Fig. 1a). Because 50 mM of NaB was not relevant to any biological system, we speculated that the detection of subG1 population was due to the drug toxicity.

Incubation of HCT116 cells with 1.0 mM NaB and HeLa cells with 10 mM NaB for 5 days resulted in morphologic changes. These changes included an enlarged, flattened shape, increased cytoplasmic to nuclear ratio, and decreased cell density accompanied by SA-β-gal staining (Fig. 4b, Supplementary Fig. 1b).

p21 expression levels in 20 MOI Ad-p21F-infected cells were similar to those in 1.0 mM NaB-treated HCT116 cells, and levels in 40 MOI Ad-p21-F-infected cells were similar to those in 2–5 mM-NaB treated cells (Fig. 4c). These results demonstrate that treatment with a low concentration of NaB induces senescence through a low level of p21 expression, but a high concentration of NaB induces apoptosis through a high level of p21 expression in HCT116 cells. In HeLa cells, apoptosis was not induced even with a high concentration of NaB. These results were consistent with previously described data on the p21 overexpression system by Ad-p21 infection.

Increased ROS levels in NaB-induced senescence and apoptosis of cancer cells. To investigate the contribution of ROS to senescence or apoptosis of HCT116 cells triggered by the treatment with different concentrations of NaB, we measured ROS levels as described above. FACS analysis of APF-stained cancer cell lines revealed a progressive increase in ROS levels following NaB treatment. The levels of ROS were increased following treatment both with 1 mM of NaB (2 to 3-fold) that induced senescence in HCT116 cells and with 5 mM of NaB (5-fold) that induced apoptosis compared with no treatment in HCT116 cells (Fig. 5a). The ROS level in apoptotic cells induced by NaB was markedly higher than that in senescent cells.

To further establish whether different cell fate outcomes were due to the induced ROS level, we investigated the effect of the antioxidant NAC on the senescent phenotype. HCT116 cells were treated with 0.5 mM NaB in the presence or absence of 5 mM NAC for 5 days. The increase of cell numbers in the G2/M fraction following treatment with 0.5 mM NaB was abrogated by co-treatment with 5 mM NAC (Fig. 5b). As shown in Fig. 5(c), culture in the presence of NAC significantly suppressed the number of SA-β-gal-positive HCT116 cells (23% to 10%). This was accompanied by a decrease in the ROS level, which suggested that the induction of senescence by NaB occurred via the generation of ROS. The treatment with NAC, however, could not prevent the apoptotic induction by higher concentrations of NaB in HCT116 cells (data not shown), though the reason remains unknown.

DNA damage response (DDR) signals mediate NaB-induced cancer cell death. To clarify the association of NaB-induced cancer cell death with the DDR, we next assayed for DDR signals including ATM and its downstream signals. One of the first processes initiated by DSB (double strand break) is massive phosphorylation of the tail of the histone variant H2AX.[30] Foci of phosphorylated H2AX (γH2AX) are rapidly formed at the DSB sites and are thought to be essential for further recruitment of damage response proteins. γH2AX is dependent on the ATM protein and other members of the ATM family.[31] To examine the effect of NaB on DDR signal–related proteins, we analyzed the changes of DSB-related protein expression levels in response to NaB by immunoblotting. Incubation with 1–5 mM NaB for 48 h resulted in the accumulation of γH2AX and ATM in HCT116 cells. Downstream proteins such as p53, phosphorylated p38 MAPK, and p21 were up-regulated by 1–5 mM NaB after 48 h of incubation (Fig. 6a). In HCT116 cells, the levels of the DSB marker γH2AX were enhanced about 20 times when apoptosis was induced by incubating with 2 mM NaB and about 3.6 times when senescence was induced by 0.5–1.0 mM NaB for 24 h compared with the control (Fig. 6b).

Discussion

In this study, we obtained the following evidence. Ad-p21F and -N infections and NaB treatment are able to induce senescence

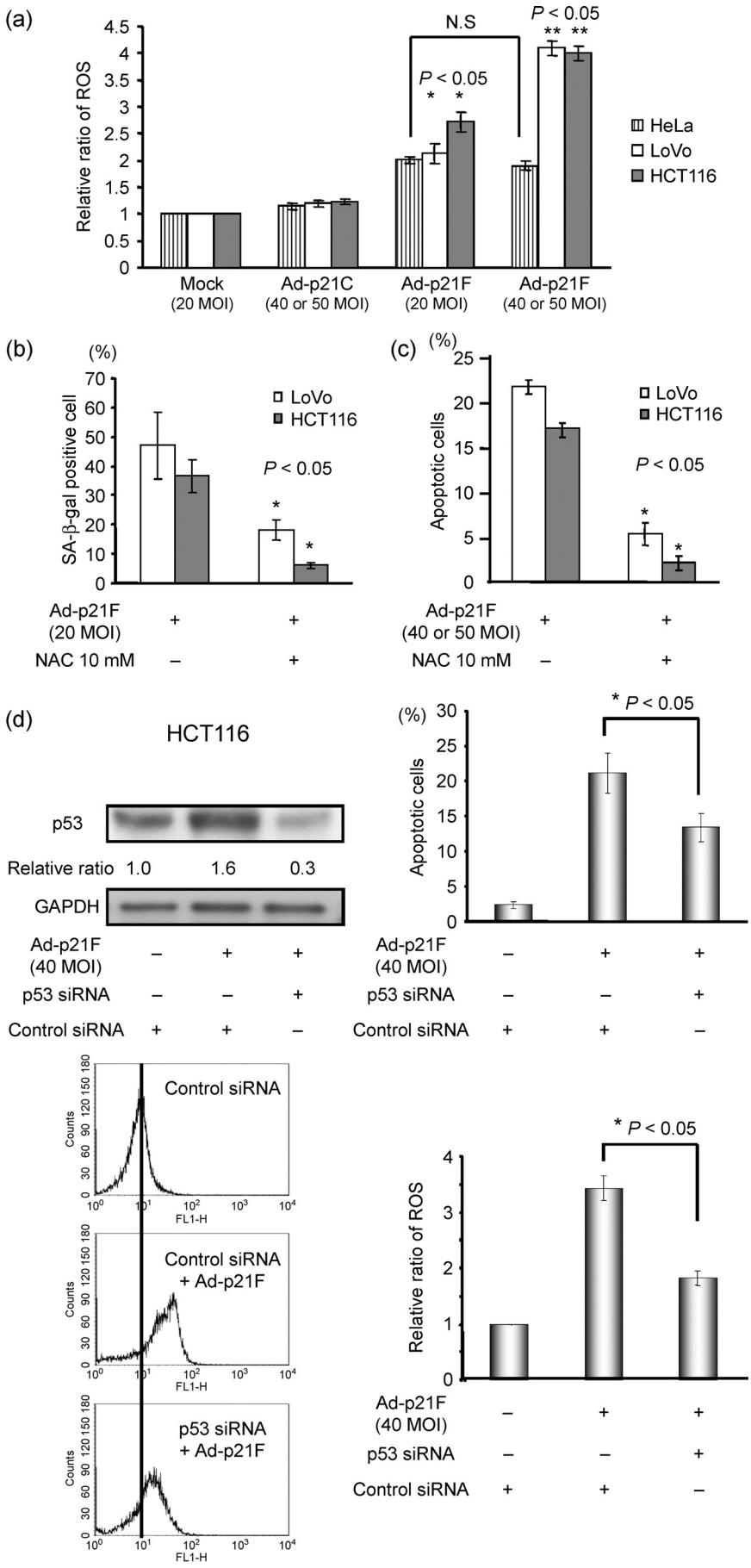

Fig. 3. Reactive oxygen species (ROS) levels in cancer cell lines in response to p21 expression levels. (a) ROS levels were evaluated by FACS analysis after staining HeLa, LoVo and HCT116 cells with the aminophenyl fluorescein (APF) fluorescent probe. Relative ratio of the geometric mean that is the average of the logarithm of the linear value for events expressed as the anti-log in Ad-p21C- (40 MOI) and Ad-p21F (20 MOI or 40 MOI)-infected cells as compared to the control (20 MOI). Generated ROS levels were significantly higher in the cancer cells infected with 20 MOI Ad-p21F than in controls and 40–50 MOI Ad-p21C-infected cells, $*P < 0.05$. In LoVo and HCT116 cells, generated ROS levels were significantly higher in the cancer cells infected with 40–50 MOI Ad-p21F than those in 20 MOI Ad-p21F-infected cells, $**P < 0.05$. Apoptosis was induced in the former and senescence in the latter. (b) Senescence induced by p21-overexpression was inhibited by *N*-acetyl-L-cystein (NAC) (ROS scavenger). LoVo and HCT116 cells were cultured in 10 mM NAC and were infected with 20 MOI Ad-p21F. The ratio of senescence-associated β-galactosidase (SA-β-gal)-positive cells after 74 h of the infection was significantly decreased in the presence of NAC. Results represent mean values of three experiments, and the error bar shows the SD. (c) Induction of apoptosis with 50 MOI Ad-p21F was also inhibited by the addition of NAC in LoVo and HCT116 cells, as indicated by the significant decrease of the subG1 fraction. Results represent mean values of three experiments, and the error bars show the SD. (d) p53-siRNA inhibited apoptotis induction by p21. Western blot analysis of p53 expression in lysates from Ad-p21F (40 MOI)-infected HCT116 cells in the absence or presence of control-siRNA and p53-siRNA is shown. Induction of apoptosis by p21 was suppressed by p53-siRNA in HCT116 cells, as indicated by the significant decrease in the subG1 fraction (upper graph). The shift to the right due to increased fluorescence corresponds to an increase in the intracellular levels of ROS. The black line indicates the mean fluorescence values in the control siRNA treated cells (lower left figure). The ROS level was significantly decreased in the presence of p53-siRNA ($P < 0.05$) (lower right graph). Results represent mean values of three experiments, and the error bar shows the SD.

doi: 10.1111/j.1349-7006.2009.01166.x

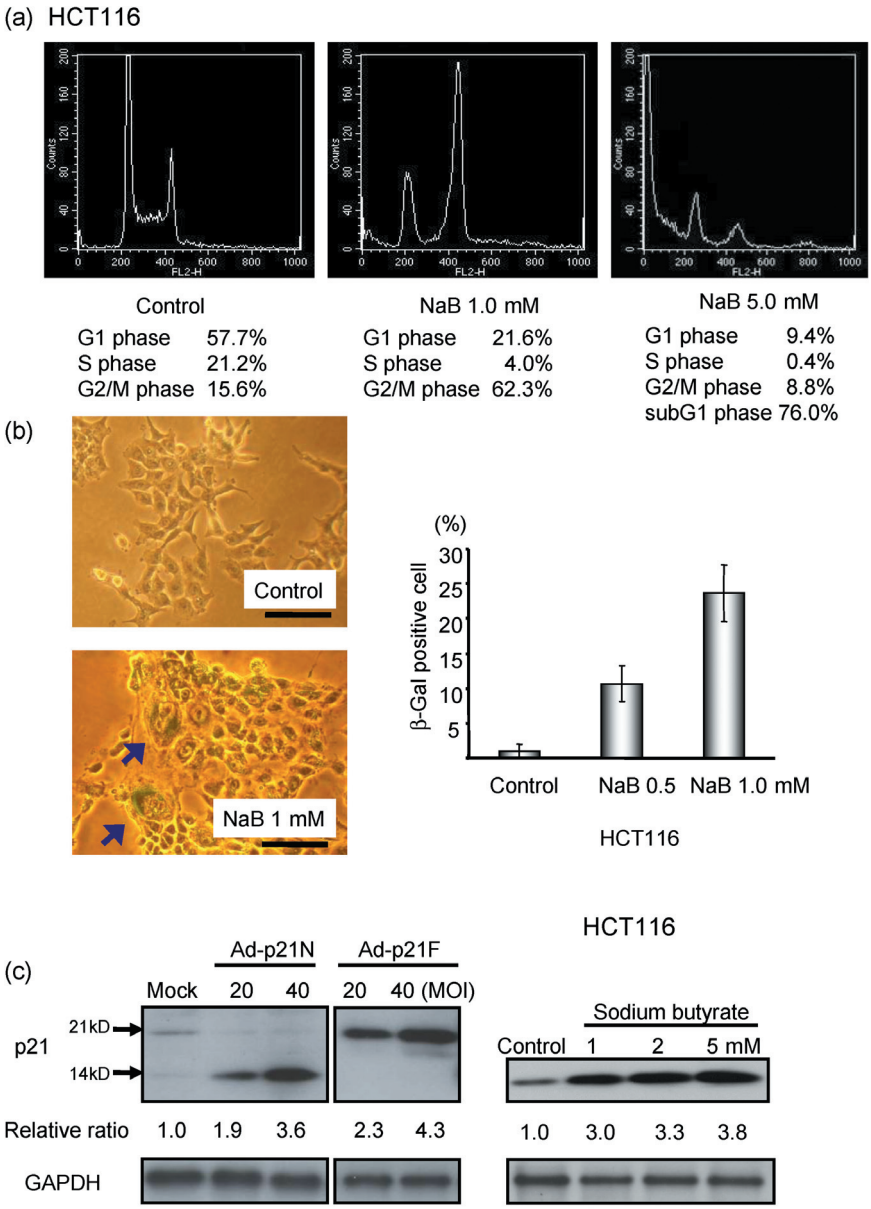

Fig. 4. (a) Effect of sodium butyrate (NaB) on cell cycle analysis and the induction of cell death. DNA contents of HeLa and HCT116 cells with or without NaB for 24 h were analyzed by flow cytometry. NaB treatment reduced the percentage of cells in the S phase and triggered the accumulation of cells in the G2/M phase in HCT116 treated with 1.0 mM NaB. (b) Treatment with 1.0 mM NaB induced morphological change in HCT116 cells that included enlargement and flattening as well as an increase in the number of senescence-associated β-galactosidase (SA-β-gal)-positive cells (arrows). Bar = 10 μM. (c) Western blot of p21 expression levels in HCT116 cell lysates from mock-, Ad-p21N-, or Ad-p21F-transfected cells with different MOIs compared to NaB-treated cells at different concentrations.

or apoptosis in cancer cell lines. The magnitude of ROS induced by p21 was critical for the p21-mediated cell fate decision. Further, the p21/ROS/p53 feedback signaling pathway is able to influence to some extent cell fate in the presence of wild-type p53. These findings help account for the differences in the p21-mediated cell fate decisions observed in various studies.

The involvement of p21 and its precise function downstream of p53 in these cell fate decisions remain elusive. p21 is capable of inhibiting CDK, which are key regulators of the cell cycle. It also inhibits DNA replication by binding PCNA, an essential DNA replication factor. p21 inhibits cell cycle progression in both G1 and G2 through inhibiting several CDK as well as PCNA.[23,24] These functions, which are carried out by different p21 domains, are each sufficient to cause growth arrest. A mutant p21-lacking PCNA-binding domain has been reported to retain the ability to achieve growth-arrest specifically in G1. This finding implies that PCNA binding is required for the maintenance of the p21-mediated G2 arrest function.[32] However, the present study clearly demonstrated that the CDK inhibitory activity in the conserved N-terminal domain is required for cancer cell death induction.

The present study clearly revealed that p21 up-regulation results in the increase of ROS levels in the cancer cells lines examined here. NAC, an inhibitor of ROS, was able to block ROS generation in response to Ad-p21F and -N infection or NaB treatment, and reduced the effect of p21 up-regulation on cell cycle inhibition and morphological changes. NAC also inhibited SA-β-gal staining of NaB treatment or Ad-p21-infected cells and protected the cells from the permanent growth-arrest phenotype. All of these findings suggest a strong relationship between oxidative damage and cancer cell senescence downstream of p21. It has also been proposed that p21 can function as a direct modulator of transcription independently of its CDK inhibition properties. We observed here that the CDK binding domain of p21, but not the PCNA binding domain, was able to generate ROS in cancer cells. Our approach to identify candidate genes which may influence ROS generation in response to p21 further delineated the pleiotropic functions of p21 associated with cancer cell death.

We showed that cancer cell fate was determined by differences in the level of ROS accumulation. In addition, the present results suggest the existence of a threshold of cellular oxidation, above

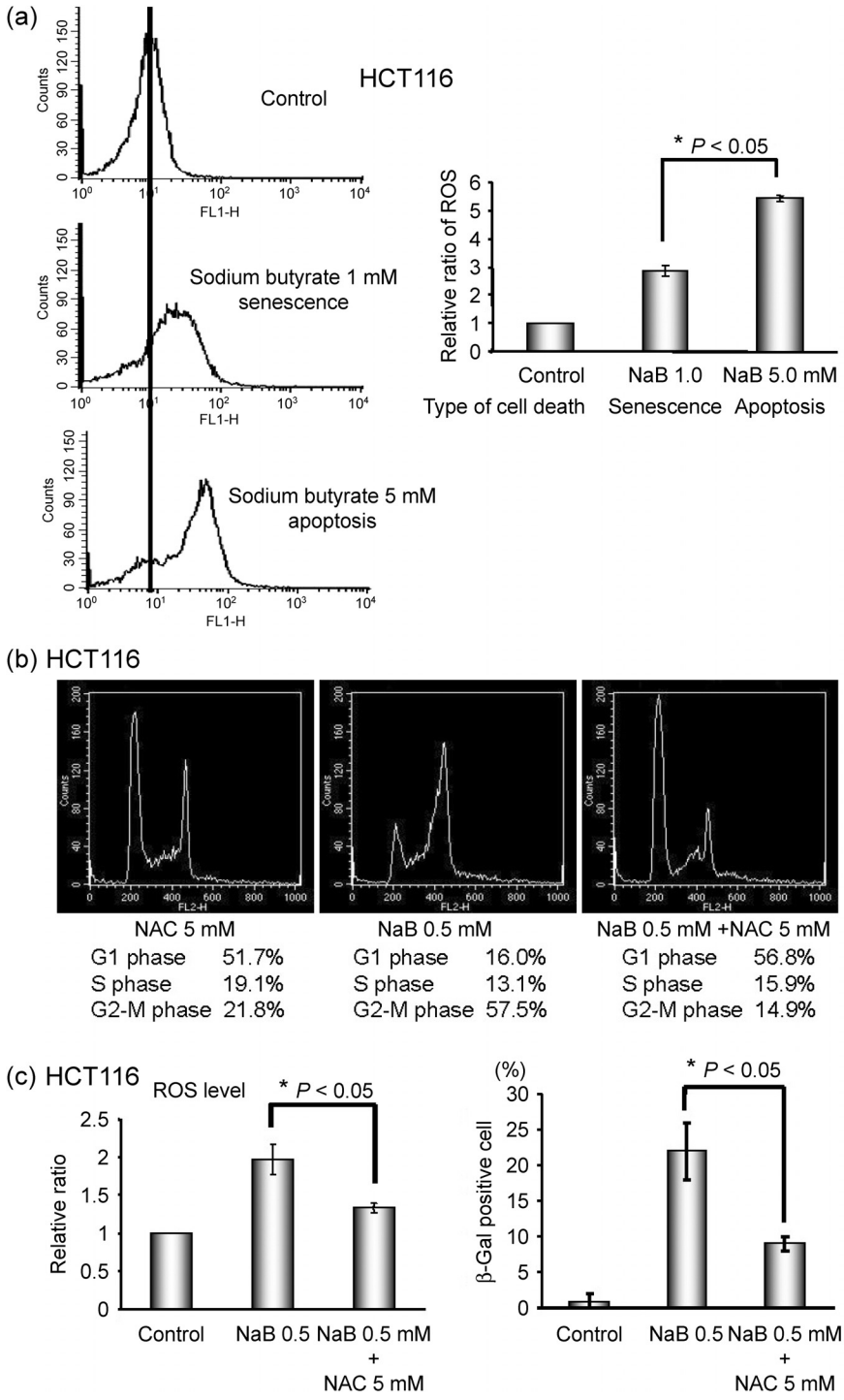

Fig. 5. Enhancement of reactive oxygen species (ROS) levels in cancer cell lines in response to sodium butyrate (NaB). (a) ROS levels were evaluated by FACS analysis after staining HCT116 cells with the aminophenyl fluorescein (APF) fluorescent probe. The ROS levels in apoptotic cells treated with 1.0 mM NaB are significantly higher than those in senescent cells induced by 5.0 mM NaB ($P < 0.05$). Data represent the average of three independent experiments and SD are indicated by error bars. (b) Treatment of *N*-acetyl-L-cystein (NAC) reduced the proportion of cells accumulating in the G2/M phase and the ratio of senescent cells following NaB treatment. HCT116 cells were cultured with 0.5 mM NaB in the presence or absence of 0.5 mM NAC for 24 h. (c) ROS level (left graph) and the ratio of senescent cells (right graph) after 96 h of treatment significantly decreased in the presence of NAC ($P < 0.05$) compared to when NAC was absent. Results represent the mean values of three experiments, and the error bars show the SD.

which the apoptotic program is initiated. Cancer cell senescence may be triggered via a lower magnitude of ROS accumulation; in turn, apoptotic cell death may be induced via a higher magnitude of ROS accumulation. It is known that the excessive generation of ROS results in the accumulation of DNA damage, in turn leading to the elimination of damaged cells. The threshold of cellular oxidation may vary between cell types or as a function of other physiological factors. However, the level of ROS accumulation in response to p21 may be a major determinant in the activation of p53-dependent apoptotic signaling. These findings provide a rationale for identifying therapeutic agents that activate p21 and selectively enhance ROS generation downstream of p21.

Acknowledgments

We would like to express our appreciation to T. Furui (Kyushu University) for the p21 deletion mutant. This work was partly supported by grants from the Japanese Ministry of Education, Culture, Sports, Science and Technology (nos. 14104014, 15390508 and 21791562).

doi: 10.1111/j.1349-7006.2009.01166.x

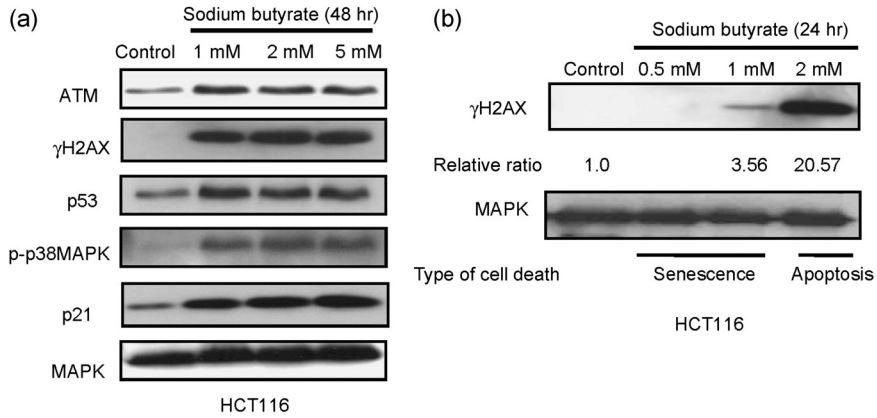

Fig. 6. Sodium butyrate (NaB) induced the expression of proteins associated with double strand break (DSB). (a) Western blot of ataxia telangiectasia mutated (ATM), phosphorylated H2AX (γH2AX), p53, phosphorylated p38 MAPK, p21, and MAPK after treatment with NaB for 48 h. (b) The level of γH2AX protein in cells treated with 2.0 mM NaB for 24 h was higher than in cells treated with 1.0 mM NaB, a level which induced senescence. Levels of γH2AX associated with the type determination of cell death.

References

1 Vaziri H, West MD, Allsopp RC *et al*. ATM-dependent telomere loss in aging human diploid fibroblasts and DNA damage lead to the posttranslational activation of p53 protein involving poly (ADP-ribose) polymerase. *EMBO J* 1997; **16**: 6018–33.
2 von Zglinicki T. Telomeres and replicative senescence: Is it only length that counts? *Cancer Lett* 2001; **168**: 111–6.
3 Di Leonardo A, Linke SP, Clarkin K, Wahl GM. DNA damage triggers a prolonged p53-dependent G1 arrest and long-term induction of Cip1 in normal fibroblasts. *Genes Dev* 1994; **8**: 2540–51.
4 Campisi J. Cellular senescence as a tumor-suppressor mechanism. *Trends Cell Biol* 2001; **11**: S27–S31.
5 Dotto G. p21 (WAF1/CIP1): more than a break to the cell cycle? *Biochim Biophys Acta* 2000; **1471**: M43–M56.
6 Alcorta DA, Xiong Y, Phelps D, Hannon G, Beach D, Barrett JC. Involvement of the cyclin-dependent kinase inhibitor p16 (INK4A) in replicative senescence of normal human fibroblasts. *Proc Natl Acad Sci U S A* 1996; **93**: 13742–7.
7 Stein GH, Drullinger LF, Soulard A, Dulic V. Differential roles for cyclin-dependent kinase inhibitors p21 and p16 in the mechanisms of senescence and differentiation in human fibroblasts. *Mol Cell Biol* 1999; **19**: 2109–17.
8 Terao Y, Nishida J, Horiuchi S *et al*. Sodium butyrate induces growth arrest and senescence-like phenotypes in gynecologic cancer cells. *Int J Cancer* 2001; **94**: 257–67.
9 Orr WC, Sohal RS. Extension of life-span by overexpression of superoxide dismutase and catalase in Drosophila melanogaster. *Science* 1994; **263**: 1128–30.
10 Chen QM, Bartholomew JC, Campisi J, Acosta M, Reagan JD, Ames BN. Molecular analysis of H2O2-induced senescent-like growth arrest in normal human fibroblasts: p53 and Rb control G1 arrest but not cell replication. *Biochem J* 1998; **332**: 43–50.
11 Hagen TM, Yowe DL, Bartholomew JC *et al*. Mitochondria decay in hepatocytes from old rats: membrane potential declines, heterogeneity and oxidants increase. *Proc Natl Acad Sci U S A* 1997; **94**: 3064–9.
12 Dumont P, Burton M, Chen QM *et al*. Induction of replicative senescence biomarkers by sublethal oxidative stress in normal human fibroblast. *Free Radical Biol Med* 2000; **28**: 361–73.
13 Lee AC, Fenster BE, Ito H *et al*. Ras protein induce senescence by altering the intracellular levels of reactive oxygen spiecies. *J Biol Chem* 1999; **274**: 7936–40.
14 Macip S, Igarshi M, Berggren P, Yu J, Lee SW, Aaroson SA. Influence of induced reactive oxygen species in p53-mediated cell gate decisions. *Mol Cell Biol* 2003; **23**: 8576–85.
15 Polyak K, Xia Y, Zweier JL, Kinzler KW, Vogelstein B. A model for p53-induced apoptosis. *Nature* 1997; **389**: 300–5.
16 Macip S, Igarshi M, Fang L *et al*. Inhibition of p21-mediated ROS accumulation can rescue p21-induced senescence. *EMBO J* 2002; **21**: 2180–8.
17 Tong B, Grimes HL, Yang T *et al*. The Gfi-1B proto-oncoprotein represses p21WAF1 and inhibits myeloid cell differentiation. *Mol Cell Biol* 1998; **18**: 2462–73.
18 Chang BD, Watanabe K, Broude EV *et al*. Effects of p21Waf1/Cip1/Sdi1 on cellular gene expression: implications for carcinogenesis, senescence, and age-related diseases. *Proc Natl Acid Sci USA* 2000; **97**: 4291–6.
19 Nakashima S, Natsugoe S, Matsumoto M *et al*. of p53 and p21 is useful for the prediction of preoperative chemotherapeutic effects in esophageal carcinoma. *Anti-Cancer Res* 2000; **20**: 1933–8.
20 Roninson I. Tumor Cell Senescence in Cancer Treatment. *Cancer Res* 2003; **63**: 2705–15.
21 Hsu SL, Chen MC, Chou YH, Hwang GY, Yin SC. Induction of p21 (CIP1/Waf1) and activation of p34 (cdc2) involved in retinoic acid-induced apoptosis in human hepatoma Hep3B cells. *Exp Cell Res* 1999; **248**: 87–96.
22 Dimri GP, Lee X, Basile G, Acosta M *et al*. A biomarker that identifies senescent human cells in culture and in aging skin *in vivo*. *Proc Natl Acad Sci U S A* 1995; **92**: 9363–7.
23 Harper JW, Elledge SJ, Keyimarsi K *et al*. Inhibition of cyclin-dependent kinases by p21. *Mol Cell Biol* 1995; **6**: 397–400.
24 Waga S, Hannon GJ, Beach D, Stillman B. The p21 inhibitor of cyclin-dependent kinases controls DNA replication by interaction with PCNA. *Nature* 1995; **369**: 574–8.
25 Waldman T, Lengauer C, Kinzlar KW, Vogelstein B. Uncoupling of S phase and mitosis induced by anticancer agent in cells lacking p21. *Nature* 1996; **381**: 713–6.
26 Deng C, Zhang P, Harper JW, Elledge SJ, Leder P. Mice lacking $p21^{CIP1/WAF1}$ undergo normal development, but are defective in G1 checkpoint control. *Cell* 1995; **82**: 675–84.
27 Tsao Y, Huang S, Chang J, Hsieh J, Pong R, Chen S. Adenovirus-mediated $p21^{(WAF1/SDII/CIP1)}$ gene transfer induces apoptosis of human cervical cancer cell lines. *J Virol* 1999; **6**: 4849–90.
28 Kagawa S, Fujiwara T, Kadowaki Y *et al*. Overexpression of the $p21^{sdi1}$ gene induces senescence-like state in human cancer cells: implication for senescence-directed molecular therapy for cancer. *Cell Death Differ* 1999; **6**: 765–72.
29 Setsukinai K, Urano Y, Kakinuma K, Majima HJ, Nagano T. Development of novel fluorescence probes that can reliably detect reactive oxygen species and distinguish specific species. *J Biol Chem* 2003; **278**: 3170–5.
30 Redon C, Pilch D, Rogakou E, Sedelnikova O, Newrock K, Bonner W. Histone H2A variants H2AX and H2AZ. *Curr Opin Genet Dev* 2002; **12**: 162–9.
31 Hammond EM, Dorie MJ, Giaccia AJ. ATR/ATM targets are phosphorylated by ATR in response to hypoxia and ATM in response to reoxygenation. *J Biol Chem* 2003; **278**: 12207–13.
32 Ando T, Kawabe T, Ohara H, Ducommun B, Itoh M, Okamoto T. Involvement of the interaction between p21 and proliferating cell nuclear antigen for the maintenance of G2/M arrest after DNA damage. *J Biol Chem* 2001; **276**: 42971–7.

Supporting Information

Additional Supporting Information may be found in the online version of this article:

Fig. S1. (a) In HeLa cells treated with 10 mM sodium butyrate (NaB), the S phase fraction was reduced and accumulated in G0/G1. Treatment of both cell types with a higher concentration of NaB induced accumulation in the subG1 phase fraction. (b) Treatment with 10 mM NaB induced morphological changes in HeLa cells that included enlargement and flattening as well as an increase in the number of senescence-associated β-galactosidase (SA-β-gal)-positive cells. Data represent the average of three independent experiments and SD are indicated by error bars. Bar = 10 μM